Supplementary Materials for Zeng et al.

Supplementary Methods

Sample preparation for flow cytometry

50 ul peripheral blood (PB) was obtained from the tail vein of mice. Red blood cells (RBCs) were lysed with 1ml RBC lysing buffer containing ammonium chloride (Biogems) for 5 minutes at room temperature (RT) and then cells were washed once with 2 ml FACS buffer (2%FBS, 2mM EDTA in PBS), 400g, 4°C, 5 min.

White blood cells (WBC) from bone marrow (BM) were harvested by flushing femora and tibiae with 3 ml FACS buffer. RBC were lysed with 3ml of RBC lysing buffer (Biogems) for 10 min on ice and then cells were washed once with 5 ml FACS buffer, 400g, 4°C, 5 minutes. Cell Debris was removed by filtration through 70 μm filters (BD Biosciences).

Staining for flow cytometry

Cells were stained with antibodies labeled with fluorochromes for 30 minutes at RT as follows. Hematopoietic populations were identified by multicolor flow cytometer (BD Fortessa) or sorted by flow cytometer cell sorter (BD FACSAria II SORP). Data were analyzed using FlowJo V7 software.

Cell markers used for flow cytometry:

Cell type	Markers
Myeloid cell	$CD11b^+$
Granulocyte	$CD11b^+$ $Gr\text{-}1^+$
B cell	$CD11b^-$ $B220^+$
Total T cell	$CD11b^-$ $CD3^+$
$CD4^+$ T cell	$CD11b^-$ $CD3^+$ $CD4^+$
$CD8^+$ T cell	$CD11b^-$ $CD3^+$ $CD8^+$
Hematopoietic stem and progenitor cell (HSPC)	Lin^- $Sca1^+$ $cKit^+$
Long term hematopoietic stem cell (LT-HSC)	Lin^- $Sca1^+$ $cKit^+$ $CD34^-$ $CD135^-$
Short term hematopoietic stem cell (ST-HSC)	Lin^- $Sca1^+$ $cKit^+$ $CD34^+$ $CD135^-$
Multipotent progenitor (MPP)	Lin^- $Sca1^+$ $cKit^+$ $CD34^+$ $CD135^+$
Common lymphoid progenitor (CLP)	Lin^- $CD127^+$ $Sca1^{med}$ $cKit^{med}$
Common myeloid progenitors (CMP)	Lin^- $CD127^-$ $Sca1^-$ $cKit^+$ $CD34^+$ $CD16/32^-$
Granulocyte/monocyte progenitors (GMP)	Lin^- $CD127^-$ $Sca1^-$ $cKit^+$ $CD34^+$ $CD16/32^+$
Megakaryocyte/erythroid progenitors (MEP)	Lin^- $CD127^-$ $Sca1^-$ $cKit^+$ $CD34^-$ $CD16/32^-$

Antibodies used for flow cytometry:

Antibody	Source	Identifier
CD45.1 PERCP-CY5.5	BD Pharmingen	560580
CD45.2 V450	BD Pharmingen	560697
Gr-1 APC	BD Pharmingen	560599
CD11b FITC	BD Pharmingen	557396
B220 PE	BD Pharmingen	553089
CD3 BV510	BD Pharmingen	563024
CD4 R718	BD Pharmingen	566939
CD8 PE-CF594	BD Pharmingen	562283
LIN PERCP-CY5.5	BD Pharmingen	561317
CD127 BV711	BD Pharmingen	565490
CD117 PE-CY7	BD Pharmingen	558163

Ly-6A/E FITC	BD Pharmingen	557405
CD34 Alexa Fluor® 647	BD Pharmingen	560230
CD16/32 V450	BD Pharmingen	560539
CD135 PE	BD Pharmingen	553842
CD45 BV510	BD Pharmingen	563891
CD45.2 BV510	BD Pharmingen	740131
Anti-Brdu PE	Biolegend	339812
CD135 BV421	BD Pharmingen	562898
Annexin V PE	Biolegend	640908

Annexin V staining of HSCs

BM cells were stained with the cocktail of FACS antibodies for 30 minutes as described above. After washing with FACS buffer, cells were resuspended in 200 μl Annexin V buffer and strained with PE-Annexin V antibody.

BrdU incorporation assay of HSCs

For detecting cell proliferation, mice were injected intraperitoneally with the 2.0% BrdU solution (Peprotech) at 0.1 mg/g body weight in PBS, once a day, for 2 days, starting before being killed for analysis. BM cells were collected and stained with anti-BrdU antibody combining with the plasma membrane marker antibodies.

Colony forming unit assay

Murine purified LT-HSCs by FACS (Lin^- $Sca1^+$ $cKit^+$ $CD34^-$ $CD135^-$) were cultured in methylcellulose (MethoCult M3434, Stemcell Technologies). Three hundred LT-HSCs per well were incubated at 37°C, 5% CO_2 for 7 days before colonies were counted.

Transplantation assay

Total BM transplantation: Competitive reconstitution assays were performed by intravenous transplantation of 2×10^5, 7.5×10^4, or 2.5×10^4 donor-derived whole bone marrow cells (CD45.2), together with 2×10^5 rescue cells (CD45.1) into irradiated ptprc CD45.1 recipient mice. Radiation dose was 9 Gy split in 2 doses 4 hours apart. For secondary transplantation, primary transplant recipients were sacrificed at 4 months post primary transplantation and 1×10^6 BM cells were 1 to 1 transplanted into irradiated secondary recipient mice. CRU frequencies in primary and secondary transplantation were assessed by ELDA software [1]. Successful engraftment was defined as the presence of a distinct $CD45.2^+CD45.1^-$ population ≥ 5% of total hematopoietic cells in peripheral blood.

HSC transplantation: For competitive HSC reconstitution assays, 200 HSCs (CD45.2) were sorted from donor bone marrow cells and transplanted into irradiated CD45.1 recipients together with 2×10^5 rescue cells (CD45.1). Radiation dose was 9 Gy split in 2 doses 4 hours apart. Donor chimerism was determined by flow cytometry every 4 weeks for 16 weeks.

Quantification of cytokines in BM serum

The femurs and tibias were flushed out with 1.5 ml PBS. After 10 min of centrifugation at 13,000 rpm, the supernatant was collected and stored at -80°C. The cytokine levels in the serum were measured using multiplex bead assays from Bio-Rad Laboratories (Bio-Plex 23-plex), according to the manufacturer's instructions.

Intestinal histopathology

Intestinal tissues from mice were collected, fixed in 4% formaldehyde, embedded in paraffin and sectioned for histological studies. Sections (4 μm) were cut with a microtome, stained with hematoxylin and eosin (H&E). Slides were scanned and images were captured using KFBIO KF-PRO-120 digital pathology slide scanner at respective magnifications. For goblet cell counting, Paraffin-embedded intestinal sections were subjected to Periodic acid-Schiff staining and the slides were

subsequently scanned and visualized using the KFBIO KF-PRO-120 digital pathology slide scanner.

Intestinal permeability test

To assess the intestinal permeability, mice were orally gavaged with 0.3 ml of FITC-dextran in PBS (100 mg/ml). 4 hours later, plasma was collected and analyzed for fluorescence intensity at an excitation of 470 nm and emission of 520 nm.

Real-time quantitative PCR

Total RNA was isolated using Trizol (TAKARA) according to manufacturer's instructions. cDNA was synthesized using 500 ng of RNA using HiScript® II Q RT SuperMix for qPCR (Vazyme). The expressions of respective genes were analyzed using ChamQ Universal SYBR qPCR Master Mix (Vazyme). Values were then normalized to the expression of GAPDH for each sample. The following primer sets were used:

mRNA	Primer pairs	Sequencing
TNF	TNF_F	CAAATGGCCTCCCTCTCAT
	TNF_R	CTCCTCCACTTGGTGGTTTG
IL6	IL6_F	CAAAGCCAGAGTCCTTCAGA
	IL6_R	GAGCATTGGAAATTGGGGTA
IL10	IL10_F	CCCAGAAATCAAGGAGCATT
	IL10_R	GCTCCACTGCCTTGCTCTTA
IL1a	IL1a_F	CGAAGACTACAGTTCTGCCATT
	IL1a_R	GACGTTTCAGAGGTTCTCAGAG
IL4	IL4_F	GGTCTCAACCCCCAGCTAGT
	IL4_R	GCCGATGATCTCTCTCAAGTGAT
IFN-γ	IFN-γ_F	ATGAACGCTACACACTGCATC
	IFN-γ_R	CCATCCTTTTGCCAGTTCCTC
GADPH	GADPH_F	AGGTCGGTGTGAACGGATTTG
	GADPH_R	TGTAGACCATGTAGTTGAGGTCA

Single cell RNA sequencing

Sample preparation and library construction. Whole BM cells, immature hematopoietic cells (Lin^-) and hematopoietic progenitor cells (Lin^- $cKit^+$) were collected by flow cytometric sorting and admixed at a 1:1:4 ratio. Single-cell RNA-seq libraries were prepared using the Chromium Single Cell 3′ Reagent Kits v3 (10x Genomics), according to the manufacturer's instructions. After the reverse transcription step, emulsions were broken and Barcoded-cDNA was purified with Dynabeads, followed by PCR amplification. Amplified cDNA was then used for 3'gene expression library construction. For gene expression library construction, 50 ng of amplified cDNA was fragmented and end-repaired, double-size selected with SPRIselect beads, and sequenced on a NovaSeq platform (Illumia) to generate 150 bp paired-end Reads.

Raw Data Processing and Analysis. Raw data (Raw reads) of fastq files were assembled from the Raw BCL files using Illumina's bcl2fastq converter. For primary quality control with FastQC software [2], the following parameters were assessed, (1) contained N was no more than 3; (2) the proportion of base with quality value below 5 was no more than 20%; (3) adapter sequence was removed. All the downstream analyses were based on the cleaned data with high quality.

Generation and quality control of Single-Cell Transcriptomes. Raw reads were demultiplexed and mapped to the reference genome by 10X Genomics Cell Ranger pipeline using default parameters. For each gene and each cell Barcode (filtered by CellRanger), unique molecule identifiers were counted to construct digital expression matrices. Then cells with fewer than 200 genes, greater than 6,000 genes, or with a ratio of mitochondrial genes >10% were excluded.

Dimensionality reduction and clustering analysis. R package Seurat [3] was used in the downstream analysis. The data was firstly normalized via "NormalizeData'' function and scaled via "ScaleData" function. Then "RunPCA'' function was used to

perform PCA analysis, ‘‘FindClusters’’ function was used to cluster cells with resolution = 1 and ‘‘RunUMAP’’ function was used to visualize with a 2-dimensional UMAP algorithm. In addition, ‘‘FindAllMarkers’’ function with default parameters was used to generate marker genes of different clusters.

Pseudotime analysis. Pseudotime analysis was performed with the Monocle2 package [4]. The structure of the trajectory was plotted in 2-dimensional space using the DDRTree dimensionality reduction algorithm, and the cells were ordered in pseudotime.

Identification of differentially expressed genes and functional enrichment analysis. Differential expressed genes between different groups was identified by ‘‘FindMarkers’’ function in Seurat. The significance of the difference was determined using a Wilcoxon rank-sum test ($p<0.05$). Functional enrichment analysis for each gene set was conducted by the R package clusterProfiler [5].

Cell–cell interaction analysis. Cell–cell interaction analysis was performed using the CellChat package [6]. Firstly, “computeCommunProb” function was used to compute the communication probability and infer cellular communication network for each dataset and then “compareInteractions” function was used to compare the interaction strength between two datasets. “rankNet” function was used to visualize the comparison of interaction strength in each signaling pathway and “netVisual_chord_gene” function was used to show the compare outgoing (or incoming) signaling associated with each cell population.

Data Availability. scRNA-seq sequencing data have been submitted to GEO under GEO: GSE201920.

16S rRNA sequencing

16S rRNA sequencing was performed as previously described [7]. Mice were transferred to separate, clean, empty cages for feces collection. Then, fresh fecal samples were collected into sterile cryopreservation tubes, quickly frozen in liquid nitrogen and stored at −80°C. DNA was extracted from 50-100 mg of fecal samples using the CTAB according to manufacturer’s instructions. The V3-V4 region of the prokaryotic small-subunit (16S) rRNA gene was amplified by slightly modified versions of primers 341F (5'-CCTACGGGNGGCWGCAG-3') and 805R(5'-GACTACHVGGGTATCTAATCC-3'). The PCR conditions to amplify the prokaryotic 16S fragments consisted of an initial denaturation at 98°C for 30 seconds; 32 cycles of denaturation at 98°C for 10 seconds, annealing at 54°C for 30 seconds, and extension at 72°C for 45 seconds, and then final extension at 72°C for 10 minutes. The PCR products were confirmed with 2% agarose gel electrophoresis and purified by AMPure XT beads (Beckman Coulter Genomics, Danvers, MA, USA) and quantified by Qubit (Invitrogen, USA). The amplicon pools were prepared for sequencing and the size and quantity of the amplicon library were assessed on Agilent 2100 Bioanalyzer (Agilent, USA) and with the Library Quantification Kit for Illumina (Kapa Biosciences, Woburn, MA, USA), respectively. The libraries were sequenced on NovaSeq PE250 platform.

Samples were sequenced on an Illumina NovaSeq platform according to the manufacturer's recommendations. Paired-end reads were assigned to samples based on their unique barcode and truncated by cutting off the barcode and primer sequence. Paired-end reads were merged using FLASH. Quality filtering on the raw reads were performed under specific filtering conditions to obtain the high-quality clean tags according to the fqtrim (v0.94). Chimeric sequences were filtered using Vsearch software (v2.3.4). After dereplication using DADA2, we obtained feature table and feature sequence. Alpha diversity and beta diversity were calculated by normalized to the same sequences randomly. Then according to SILVA(release 138) classifier, feature abundance was normalized using relative abundance of each sample. Blast was used for sequence alignment, and the feature sequences were annotated with SILVA database for each representative sequence.

16S rRNA sequencing data have been submitted to Sequence Read Archive (SRA): PRJNA637751.

LC-MS untargeted metabolomics

LC-MS untargeted metabolomics analysis was performed as previously described [7]. The collected samples were thawed on ice, and metabolites were extracted from 20 μL of each sample using 120 μL of precooled 50% methanol buffer. Then the mixture of metabolites was vortexed for 1 min and incubated for 10 min at room temperature and stored at -20°C overnight. The mixture was centrifugated at 4,000 g for 20 min, subsequently the supernatant was transferred to 96-well plates. The samples were stored at 80°C prior to the LC-MS analysis. Pooled quality control (QC) sample were also prepared by

combining 10 μL of each extraction mixture.

All samples were analyzed using a TripleTOF 5600 Plus high-resolution tandem mass spectrometer (SCIEX, Warrington, UK) with both positive and negative ion modes. Chromatographic separation was performed using an ultra-performance liquid chromatography (UPLC) system (SCIEX, UK). An ACQUITY UPLC T3 column (100mm*2.1mm, 1.8μm, Waters, UK) was used for the reversed-phase separation. The column temperature was maintained at 35°C. The TripleTOF 5600 Plus system was used to detect metabolites eluted from the column. The interface heater temperature was 650°C.For the positive-ion mode, the ion spray floating voltage was set at 5kV, while for the negative-ion mode, it was set at -4.5kV. The MS data were acquired in the IDA mode. The total cycle time was fixed at 0.56s. Four-time bins were summed for each scan at a pulse frequency of 11 kHz by monitoring the 40 GHz multichannel TDC detector with four-anode/channel detection. Dynamic exclusion was set for 4s. During the entire acquisition period, the mass accuracy was calibrated every 20 samples. Furthermore, a QC sample was analyzed every 10 samples to evaluate the stability of the LC-MS.

Each ion was identified by the comprehensive information of retention time and m/z. The intensity of each peak was recorded and a three-dimensional matrix containing arbitrarily assigned peak indices (retention time, m/z pairs), sample names (observations) and ion intensity information (variables) was generated. Then the information was matched to the in-house and public database. The open access databases, KEGG and HMDB, were used to annotate the metabolites by matching the exact molecular mass data (m/z) to those from the database within a threshold of 10 ppm. The peak intensity data was further preprocessed using metaX. Features that were detected in <50% of QC samples or 80% of test samples were removed, and values for missing peaks were extrapolated with the k-nearest neighbor algorithm to further improve the data quality. PCA was performed to detect outliers and batch effects using the pre-processed dataset. QC-based robust LOESS signal correction was fitted to the QC data with respect to the order of injection to minimize signal intensity drift over time. In addition, the relative standard deviations of the metabolic features were calculated across all QC samples, and those with standard deviations > 30% were removed.

The group datasets were normalized before analysis was performed. Data normalization was performed on all samples using the probabilistic quotient normalization algorithm. Then, QC-robust spline batch correction was performed using QC samples. The *P* value analyzed by student *t* tests was used for the different metabolite selection.

Administration of specific bacterial taxa in mice

Before administration of specific bacterial taxa in mice, mice were gavaged with 100 μl antibiotic cocktail for 3 days, containing 1 g/L ampicillin, 0.5 g/L neomycin, 0.5 g/l vancomycin and 1 g/l metronidazole. Then, mice were given 200 μl microbiota (5×10^8 CFU/ml) resuspended in sterile PBS daily for three weeks, starting the first day after the antibiotic treatment. An identical volume of sterile PBS was used as a vehicle control. Thereafter, mice were sacrificed at indicated time and the proportions, absolute numbers and implantation efficiency of HSCs were determined as described above.

Clostridium (CCUG #53142) were purchased from CCUG and cultured on blood agar at 37°C in an anaerobic chamber, according to the manufacturer's instructions. *Lachnospiraceae* in this study was a mixture of 23 strains that belong to the family *Lachnospiraceae* as previously reported [8, 9]. In brief, gut microbiota was collected from ceca of wild-type C57BL/6 mice in a sterile manner and immediately transferred to an anaerobic chamber. After enrichment and identification by PCR, *Lachnospiraceae* were cultured on brain heart infusion agar with 0.1% cysteine (Sigma-Aldrich), 1 mg/L aztreonam (Sigma-Aldrich) and 2 mg/L gentamicin (Sigma-Aldrich).

Administration of metabolites in mice

After 1 month of acclimatization with a standard chow diet, mice were randomly divided into 6 groups: (1) control group; (2) tryptophan group; (3) I3C group; (4) indole group (5) indole-1-acetic acid (IAA) group (6) indole-3-butyric acid group. Mice were fed their assigned diet for 4 weeks. All diets were adjusted to the same energy level, and the diet compositions in different groups are listed as follows.

Feed ingredient in different diet conditions (Ingredient g/kg diet):

Group / Ingredient	Control	Tryptophan	I3C	Indole	IAA	Indole-3-butyric acid
Corn Starch	550.5	548.5	550.5	550.5	550.5	550.5
Maltodextrin	125	125	125	125	125	125
Cellulose	50	50	50	50	50	50
Corn Oil	50	50	50	50	50	50
Mineral Mix	35	35	35	35	35	35
Sodium Bicarbonate	7.5	7.5	7.5	7.5	7.5	7.5
Vitamin Mix	10	10	10	10	10	10
Choline Bitartrate	2	2	2	2	2	2
Amino acid Mix	170	170	170	170	170	170
Tryptophan	2	4	2	2	2	2
Specific metabolite			2.5 I3C	2.5 Indole	2,5 IAA	2.5 Indole-3-butyric acid

Reference:

1. Hu, Y. and G.K. Smyth, *ELDA: extreme limiting dilution analysis for comparing depleted and enriched populations in stem cell and other assays.* J Immunol Methods, 2009. **347**(1-2): p. 70-8.
2. de Sena Brandine, G. and A.D. Smith, *Falco: high-speed FastQC emulation for quality control of sequencing data.* F1000Res, 2019. **8**: p. 1874.
3. Satija, R., et al., *Spatial reconstruction of single-cell gene expression data.* Nat Biotechnol, 2015. **33**(5): p. 495-502.
4. Trapnell, C., et al., *The dynamics and regulators of cell fate decisions are revealed by pseudotemporal ordering of single cells.* Nat Biotechnol, 2014. **32**(4): p. 381-386.
5. Wu, T., et al., *clusterProfiler 4.0: A universal enrichment tool for interpreting omics data.* Innovation (N Y), 2021. **2**(3): p. 100141.
6. Jin, S., et al., *Inference and analysis of cell-cell communication using CellChat.* Nat Commun, 2021. **12**(1): p. 1088.
7. Li, X., et al., *Tyrosine supplement ameliorates murine aGVHD by modulation of gut microbiome and metabolome.* EBioMedicine, 2020. **61**: p. 103048.
8. Reeves, A.E., et al., *Suppression of Clostridium difficile in the gastrointestinal tracts of germfree mice inoculated with a murine isolate from the family Lachnospiraceae.* Infect Immun, 2012. **80**(11): p. 3786-94.
9. Guo, H., et al., *Multi-omics analyses of radiation survivors identify radioprotective microbes and metabolites.* Science, 2020. **370**(6516).

Supplemental Figures:

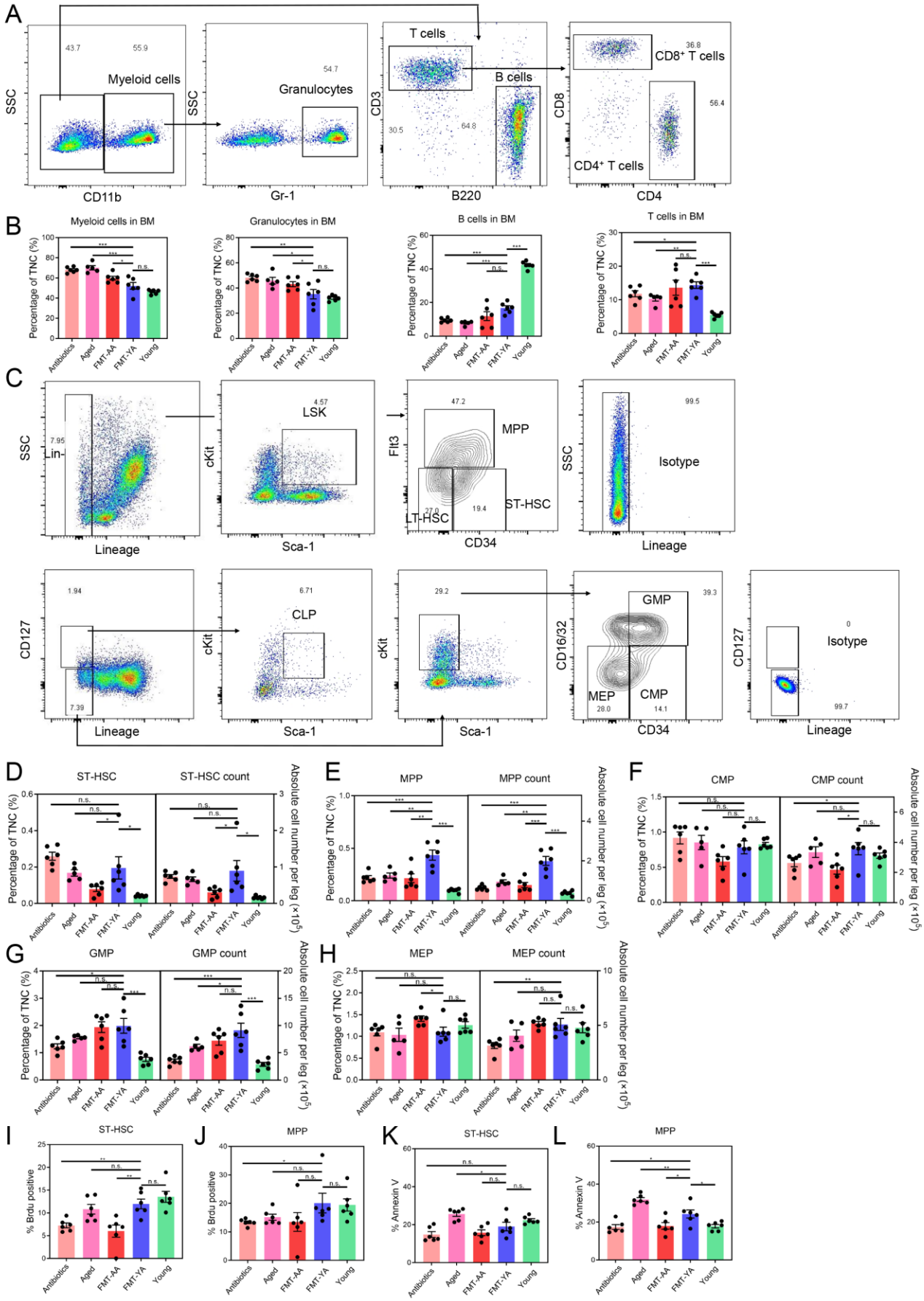

Supplemental Figure S1. Transplantation of young gut microbiota rescued defective phenotype of aged HSCs, related to Figure 1. (A) Flow cytometry gating strategy. After being discriminated from debris by gating on forward scatter (FSC) and side scatter (SSC), myeloid cells, granulocytes, $CD4^+$ T cells, $CD8^+$ T cells and B cells were identified in nucleated peripheral blood (PB) of mice. (B) Proportions of myeloid cells, granulocytes, B cells and T cells in bone marrow (BM) from aged mice treated with antibiotics (Antibiotics), normal control aged mice (Aged), aged mice gavaged with aged gut microbiota (FMT-AA), aged mice gavaged with young gut microbiota (FMT-YA) and normal control young mice (Young). (C) Flow cytometric sorting strategy for HSPCs, LT-HSCs, ST-HSCs, MPPs, CLPs, CMPs, GMPs and MEPs. (D-H) Proportions and absolute numbers of ST-HSCs, MPPs, CMPs, GMPs and MEPs in BM. (I-J) BrdU incorporation was detected by anti-BrdU antibody in ST-HSCs and MPPs. (K-L) Apoptosis was measured by Annexin V staining in ST-HSCs and MPPs. Each point represents data from a single mouse (n = 6 per group). Graphs show mean ± SEM, with statistical significance determined by student's t-test. $*P < .05$, $**P < .01$, $***P < .001$, n.s., nonsignificant.

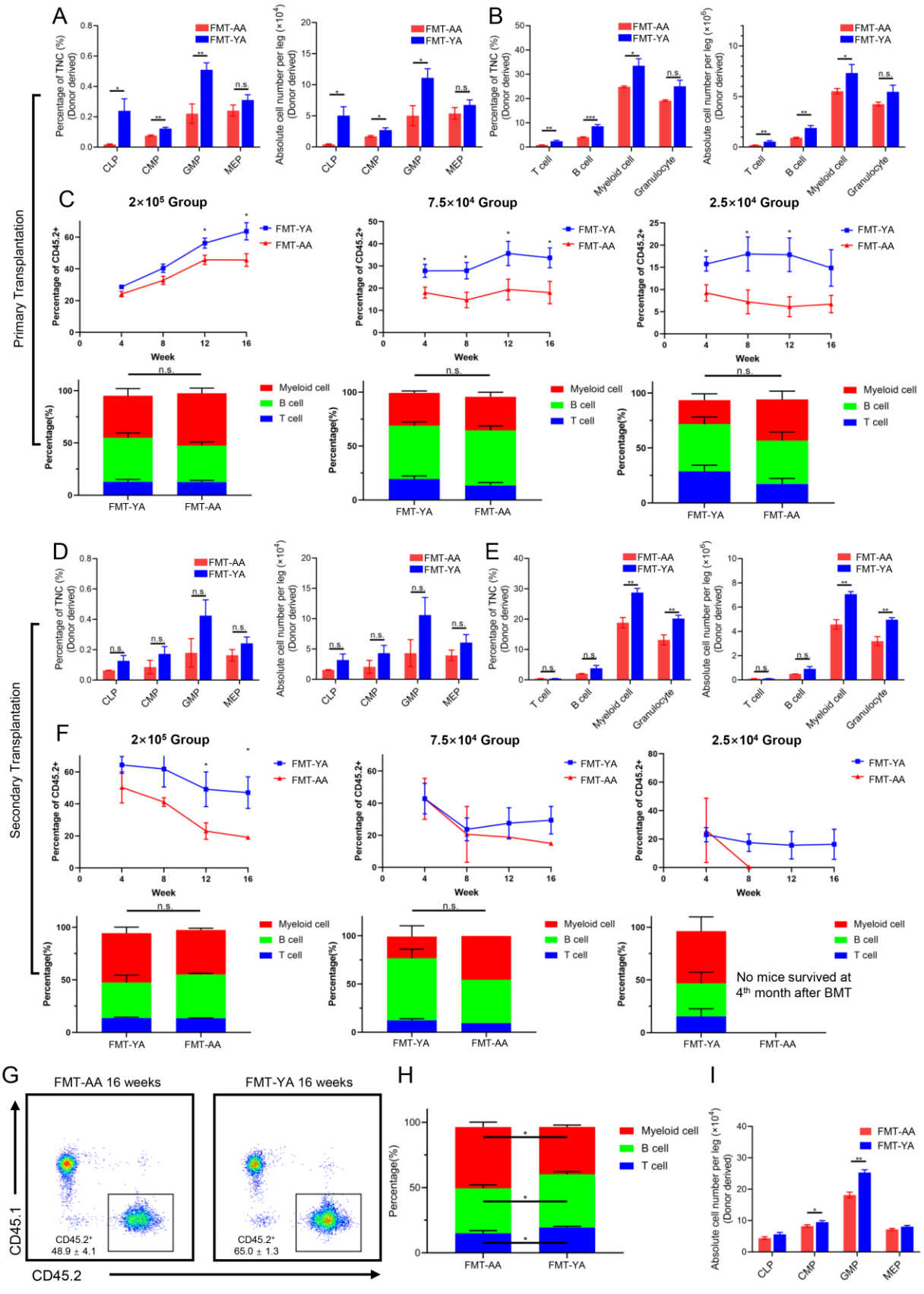
Primary Transplantation
Secondary Transplantation
A
B
C
D
E
F
G
H
I
FMT-AA
FMT-YA
Percentage of TNC (%) (Donor derived)
Absolute cell number per leg (×10⁴) (Donor derived)
Absolute cell number per leg (×10⁶) (Donor derived)
CLP
CMP
GMP
MEP
T cell
B cell
Myeloid cell
Granulocyte
n.s.
2×10⁵ Group
7.5×10⁴ Group
2.5×10⁴ Group
Percentage of CD45.2+
Week
Percentage(%)
No mice survived at 4th month after BMT
FMT-AA 16 weeks
FMT-YA 16 weeks
CD45.1
CD45.2
CD45.2⁺ 48.9 ± 4.1
CD45.2⁺ 65.0 ± 1.3

Supplemental Figure S2. Transplantation of young gut microbiota increased functional HSCs in mice, related to Figure 2. (A) The percentage and absolute cell number of donor-derived CLPs, CMPs, GMPs and MEPs in BM from recipient mice in primary LDA. (B) The percentage and absolute cell number of donor-derived T cells, B cells, myeloid cells and granulocytes in BM from recipient mice in primary LDA. (C) 2×10^5, 7.5×10^4, or 2.5×10^4 donor-derived BM cells (CD45.2), together with 2×10^5 rescue cells (CD45.1) were transplanted into irradiated ptprc CD45.1 recipient mice by intravenous injection. PB was analyzed for donor-derived $CD45.2^+$ reconstitution in recipient mice (top panels) and for proportions of mature donor-derived B cells, T cells and myeloid cells (bottom panels). (D) The percentage and absolute cell number of donor-derived CLPs, CMPs, GMPs and MEPs in BM from recipient mice in secondary LDA. (E) The percentage and absolute cell number of donor-derived T cells, B cells, myeloid cells and granulocytes in BM of the secondary recipients. (F) At 4 months post transplantation, BM cells were isolated from the primary competitive transplant recipients, and 1×10^6 BM cells were injected i.v. into lethally irradiated secondary recipient mice. PB was analyzed for donor-derived $CD45.2^+$ reconstitution in recipient mice (top panels) and for proportions of mature donor-derived B cells, T cells and myeloid cells (bottom panels). (G) Representative flow cytometry plots of donor-derived $CD45.2^+$ reconstitution in $CD45.1^+$ mice at 16 weeks post transplantation in HSC transplantation assay. (H) Proportions of donor-derived B cells, T cells and myeloid cells in PB at 4 months post HSC transplantation. (I) The absolute cell number of donor-derived CLPs, CMPs, GMPs and MEPs in BM from recipient mice in HSC transplantation assay. Graphs show mean ± SEM, with statistical significance determined by student's t-test (n = 6 per group). $*P < .05$, $**P < .01$, $***P < .001$, n.s., nonsignificant.

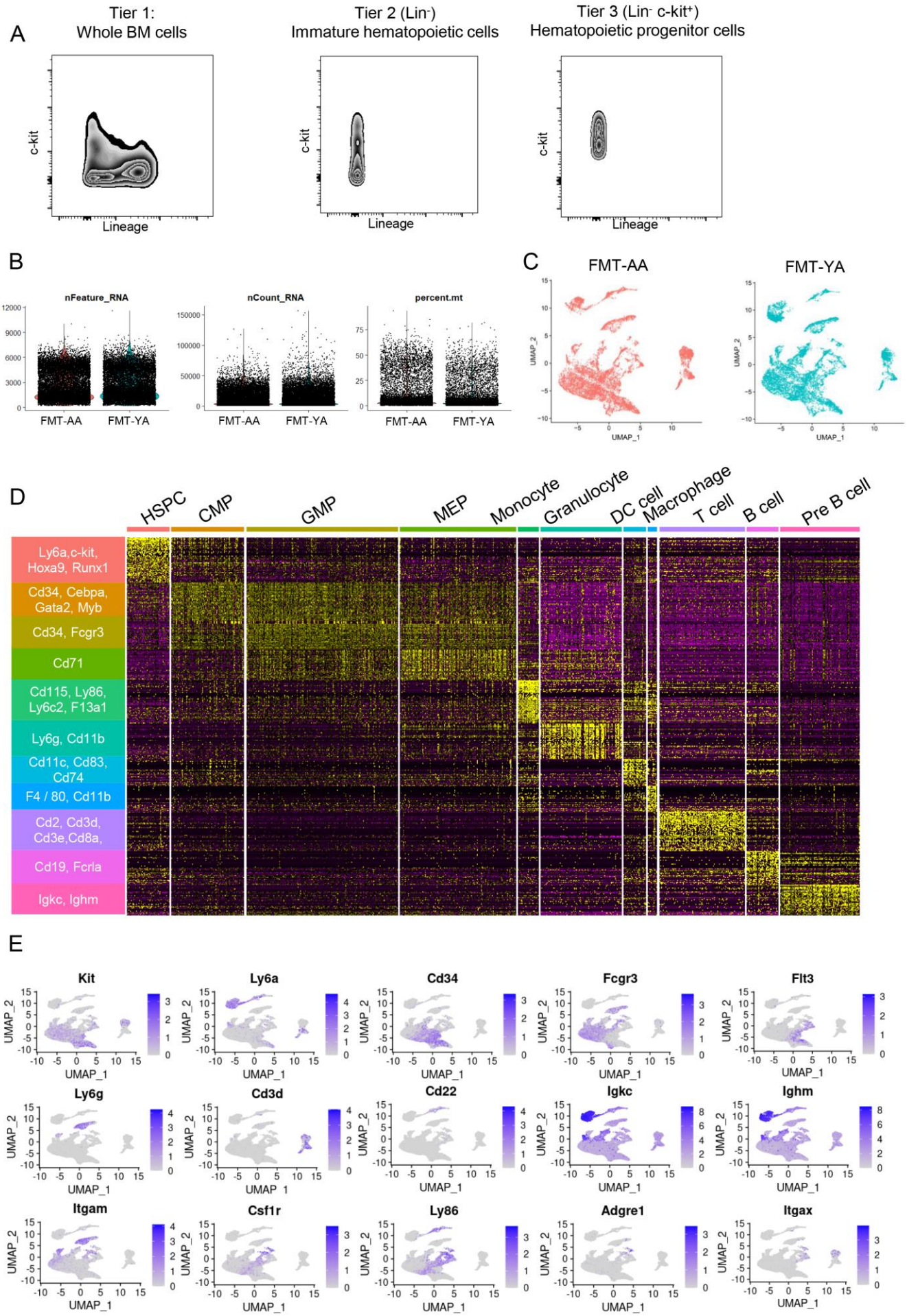
A
Tier 1:
Whole BM cells
Tier 2 (Lin-)
Immature hematopoietic cells
Tier 3 (Lin- c-kit+)
Hematopoietic progenitor cells
c-kit
Lineage
B
nFeature_RNA
nCount_RNA
percent.mt
FMT-AA
FMT-YA
C
FMT-AA
FMT-YA
UMAP_1
UMAP_2
D
HSPC
CMP
GMP
MEP
Monocyte
Granulocyte
DC cell
Macrophage
T cell
B cell
Pre B cell
Ly6a,c-kit, Hoxa9, Runx1
Cd34, Cebpa, Gata2, Myb
Cd34, Fcgr3
Cd71
Cd115, Ly86, Ly6c2, F13a1
Ly6g, Cd11b
Cd11c, Cd83, Cd74
F4 / 80, Cd11b
Cd2, Cd3d, Cd3e,Cd8a,
Cd19, Fcrla
Igkc, Ighm
E
Kit
Ly6a
Cd34
Fcgr3
Flt3
Ly6g
Cd3d
Cd22
Igkc
Ighm
Itgam
Csf1r
Ly86
Adgre1
Itgax

Supplemental Figure S3. A transcriptome-wide landscape of hematopoiesis after FMT by single cell RNA sequencing, related to Figure 3. (A) Flow cytometry illustrating the sorting scheme for the whole BM cells, immature hematopoietic cells (Lin^-) and hematopoietic progenitor cells (Lin^- $cKit^+$) for sample preparation in single cell RNA sequencing. (B) Violin plots showing the feature counts, read counts and mitochondrial counts in FMT-YA and FMT-AA samples during quality control. (C) Umap plots showing that no significant batch effects were observed between FMT-YA and FMT-AA samples. (D) Heatmap showing the most significant DEGs in different clusters. (E) Violin plots showing expression of key marker genes in different clusters. The significance of the difference was determined using a Wilcoxon rank-sum test. *$P < .05$, **$P < .01$, ***$P < .001$, n.s., nonsignificant.

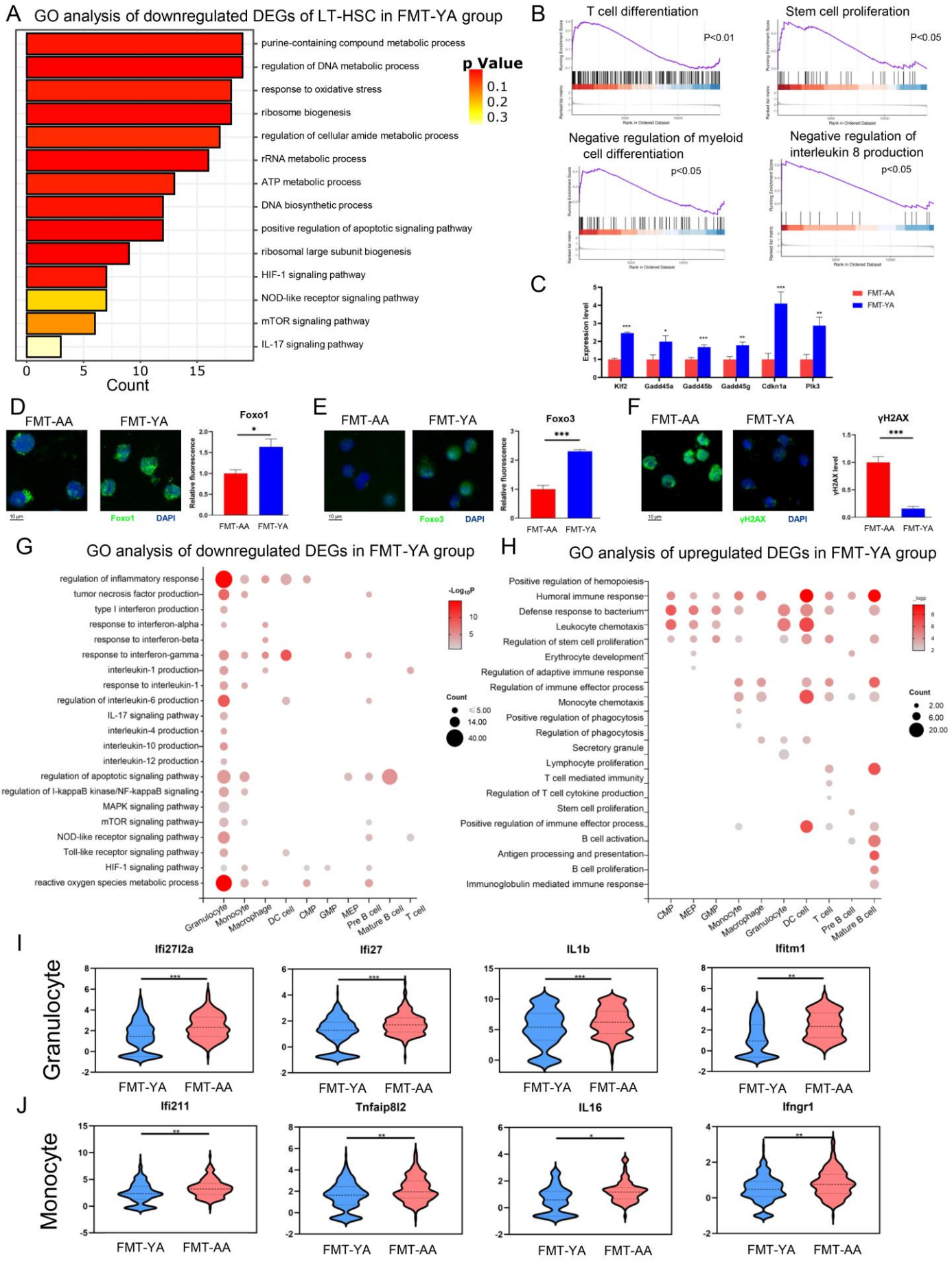
A
GO analysis of downregulated DEGs of LT-HSC in FMT-YA group
purine-containing compound metabolic process
regulation of DNA metabolic process
response to oxidative stress
ribosome biogenesis
regulation of cellular amide metabolic process
rRNA metabolic process
ATP metabolic process
DNA biosynthetic process
positive regulation of apoptotic signaling pathway
ribosomal large subunit biogenesis
HIF-1 signaling pathway
NOD-like receptor signaling pathway
mTOR signaling pathway
IL-17 signaling pathway
p Value
0.1
0.2
0.3
0
5
10
15
Count
B
T cell differentiation
P<0.01
Stem cell proliferation
P<0.05
Negative regulation of myeloid cell differentiation
p<0.05
Negative regulation of interleukin 8 production
p<0.05
C
FMT-AA
FMT-YA
Expression level
Klf2
Gadd45a
Gadd45b
Gadd45g
Cdkn1a
Pik3
D
FMT-AA
FMT-YA
Foxo1
DAPI
Foxo1
Relative fluorescence
FMT-AA
FMT-YA
E
FMT-AA
FMT-YA
Foxo3
DAPI
Foxo3
Relative fluorescence
FMT-AA
FMT-YA
F
FMT-AA
FMT-YA
γH2AX
DAPI
γH2AX
γH2AX level
FMT-AA
FMT-YA
G
GO analysis of downregulated DEGs in FMT-YA group
regulation of inflammatory response
tumor necrosis factor production
type I interferon production
response to interferon-alpha
response to interferon-beta
response to interferon-gamma
interleukin-1 production
response to interleukin-1
regulation of interleukin-6 production
IL-17 signaling pathway
interleukin-4 production
interleukin-10 production
interleukin-12 production
regulation of apoptotic signaling pathway
regulation of I-kappaB kinase/NF-kappaB signaling
MAPK signaling pathway
mTOR signaling pathway
NOD-like receptor signaling pathway
Toll-like receptor signaling pathway
HIF-1 signaling pathway
reactive oxygen species metabolic process
-Log10P
Count
≤5.00
14.00
40.00
Granulocyte
Monocyte
Macrophage
DC cell
CMP
GMP
MEP
Pre B cell
Mature B cell
T cell
H
GO analysis of upregulated DEGs in FMT-YA group
Positive regulation of hemopoiesis
Humoral immune response
Defense response to bacterium
Leukocyte chemotaxis
Regulation of stem cell proliferation
Erythrocyte development
Regulation of adaptive immune response
Regulation of immune effector process
Monocyte chemotaxis
Positive regulation of phagocytosis
Regulation of phagocytosis
Secretory granule
Lymphocyte proliferation
T cell mediated immunity
Regulation of T cell cytokine production
Stem cell proliferation
Positive regulation of immune effector process
B cell activation
Antigen processing and presentation
B cell proliferation
Immunoglobulin mediated immune response
Count
2.00
6.00
20.00
CMP
MEP
GMP
Monocyte
Macrophage
Granulocyte
DC cell
T cell
Pre B cell
Mature B cell
I
Granulocyte
Ifi27l2a
Ifi27
IL1b
Ifitm1
FMT-YA
FMT-AA
J
Monocyte
Ifi211
Tnfaip8l2
IL16
Ifngr1
FMT-YA
FMT-AA

Supplemental Figure S4. Transcriptome changes of LT-HSCs induced by FMT, related to Figure 4. (A) Representative GO analysis results enriched in downregulated DEGs of LT-HSCs in FMT-YA group. (B) Representative GSEA enrichment plots of GO terms in LT-HSCs. (C) Bar graph showing the expression levels of FoxO signaling pathway-associated genes in HSCs. (D-F) Representative images and quantification of relative fluorescence of LT-HSCs stained with an anti-Foxo1, anti-Foxo3 and anti-γH2AX antibody. (G-H) Representative GO terms and KEGG pathways enriched in DEGs of hematopoietic lineage subpopulations in BM between the FMT-YA and FMT-AA groups. (I-J) Violin plots showing the expression of inflammation-related genes in granulocytes and monocytes.

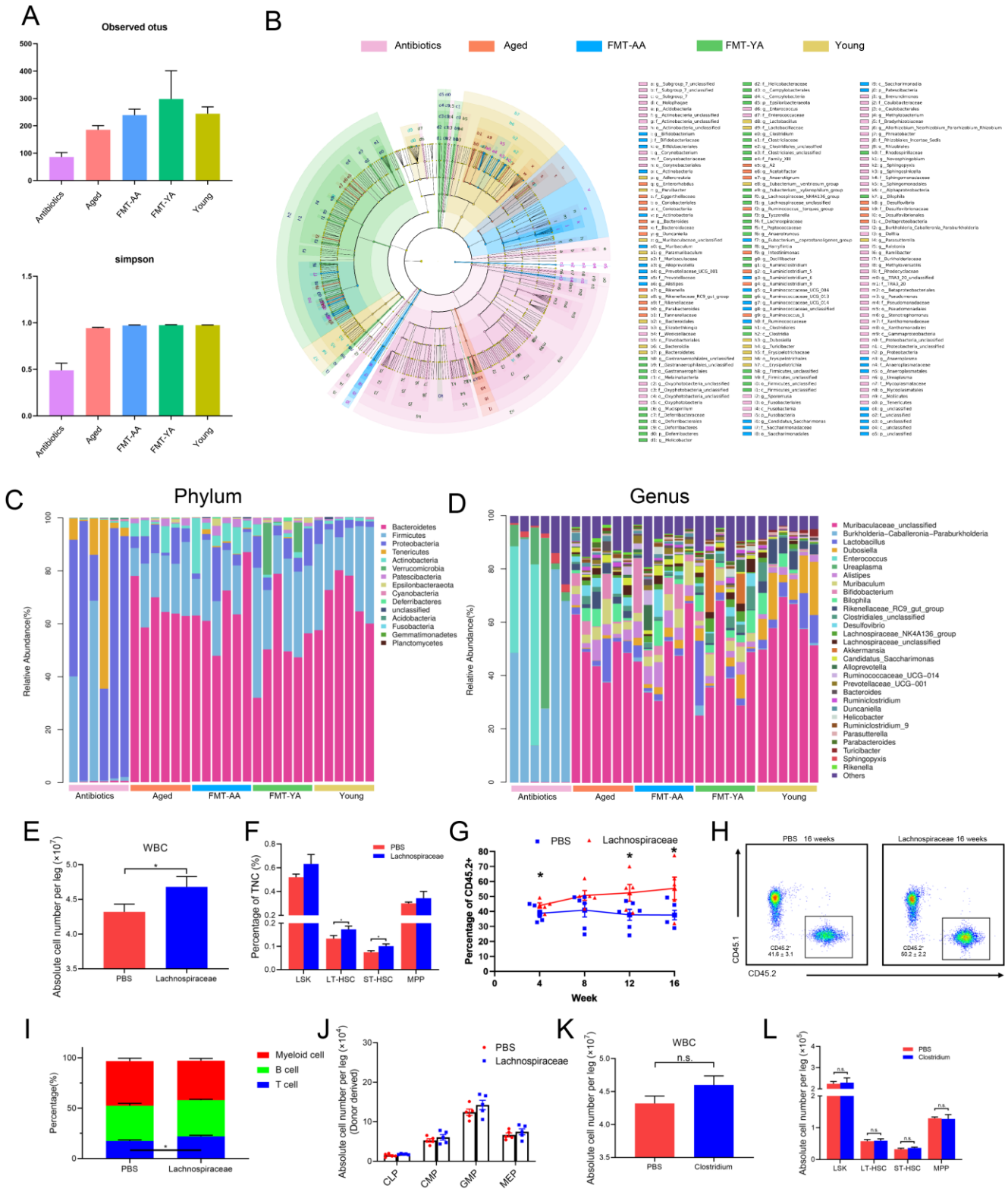
A
Observed otus
simpson
Antibiotics
Aged
FMT-AA
FMT-YA
Young
B
C
Phylum
Relative Abundance(%)
Bacteroidetes
Firmicutes
Proteobacteria
Tenericutes
Actinobacteria
Verrucomicrobia
Patescibacteria
Epsilonbacteraeota
Cyanobacteria
Deferribacteres
unclassified
Acidobacteria
Fusobacteria
Gemmatimonadetes
Planctomycetes
D
Genus
Muribaculaceae_unclassified
Burkholderia−Caballeronia−Paraburkholderia
Lactobacillus
Dubosiella
Enterococcus
Ureaplasma
Alistipes
Muribaculum
Bifidobacterium
Bilophila
Rikenellaceae_RC9_gut_group
Clostridiales_unclassified
Desulfovibrio
Lachnospiraceae_NK4A136_group
Lachnospiraceae_unclassified
Akkermansia
Candidatus_Saccharimonas
Alloprevotella
Ruminococcaceae_UCG−014
Prevotellaceae_UCG−001
Bacteroides
Ruminiclostridium
Duncaniella
Helicobacter
Ruminiclostridium_9
Parasutterella
Parabacteroides
Turicibacter
Sphingopyxis
Rikenella
Others
E
WBC
Absolute cell number per leg (×10^7)
PBS
Lachnospiraceae
F
Percentage of TNC (%)
LSK
LT-HSC
ST-HSC
MPP
G
Percentage of CD45.2+
Week
H
PBS 16 weeks
Lachnospiraceae 16 weeks
CD45.1
CD45.2
I
Percentage(%)
Myeloid cell
B cell
T cell
J
Absolute cell number per leg (×10^4) (Donor derived)
CLP
CMP
GMP
MEP
K
WBC
n.s.
Clostridium
L
Clostridium
LSK
LT-HSC
ST-HSC
MPP

Supplemental Figure S5. FMT effectively modulated the gut microbiome in recipient mice, related to Figure 6. (A) Alpha diversity (Observed otus and Simpson index) of bacterial communities in Antibiotics, Aged, FMT-AA, FMT-YA and Young mice (n=6 per group). (B) Taxonomic cladogram obtained from LEfSe analysis showing differential bacterial taxa among five groups. Pink indicated increased abundance clusters in Antibiotics group; Red indicated increased abundance clusters in Aged group; Blue indicated increased abundance clusters in FMT-AA group; Green indicated increased abundance clusters in FMT-YA group; Yellow indicated increased abundance clusters in Young group. (C) Relative abundance of microbiota at the phylum level among five groups (n=6 per group). (D) Relative abundance of microbiota at the genus level among five groups (n=6 per group). (E) Count of WBCs in BM in control group vs *Lachnospiraceae* group (n=5 per group). (F) Proportions of HSPCs in BM in control group vs *Lachnospiraceae* group (n=5 per group). (G) Donor-derived $CD45.2^+$ reconstitution in $CD45.1^+$ mice at 16 weeks post WBM competitive transplantation (n=5 per group). (H) Representative flow cytometry plots of donor-derived $CD45.2^+$ reconstitution in $CD45.1^+$ mice in HSC transplantation assay. (I) Proportions of donor-derived B cells, T cells and myeloid cells in PB at 4 months post HSC transplantation (n=5 per group). (J) The absolute cell number of donor-derived CLPs, CMPs, GMPs and MEPs in BM from recipient mice in HSC transplantation assay (n=5 per group). (K) Absolute number of TNCs in BM in control group vs *Clostridium* group (n=5 per group). (L) Absolute number of HSPCs in BM in control group vs *Clostridium* group (n=5 per group). Graphs show mean ± SEM, with statistical significance determined by unpaired student's t-test. $*P < .05$, n.s., nonsignificant.

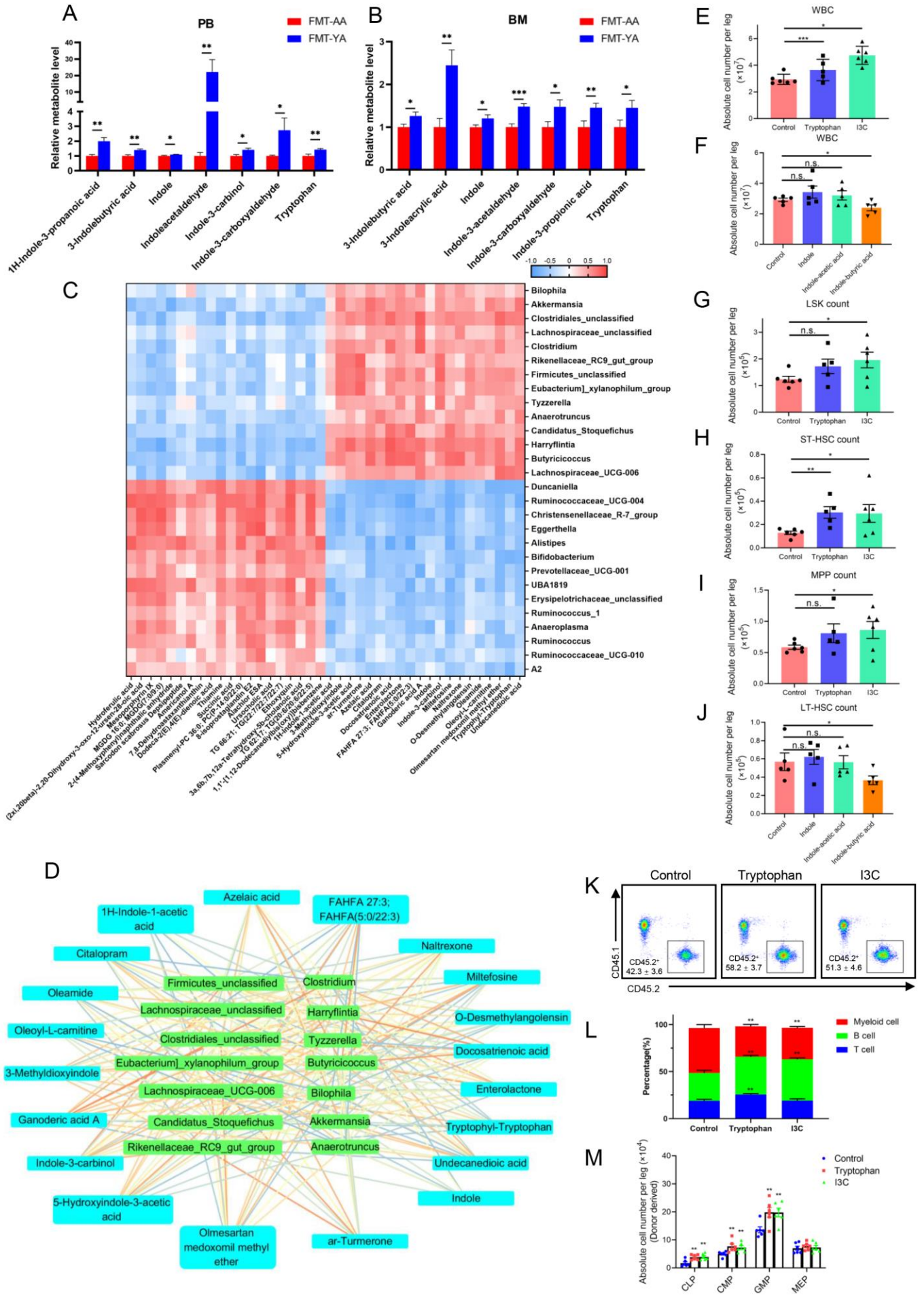
A
PB
FMT-AA
FMT-YA
Relative metabolite level
1H-Indole-3-propanoic acid
3-Indolebutyric acid
Indole
Indoleacetaldehyde
Indole-3-carbinol
Indole-3-carboxyaldehyde
Tryptophan
B
BM
FMT-AA
FMT-YA
Relative metabolite level
3-Indolebutyric acid
3-Indoleacrylic acid
Indole
Indole-3-acetaldehyde
Indole-3-carboxyaldehyde
Indole-3-propionic acid
Tryptophan
C
Bilophila
Akkermansia
Clostridiales_unclassified
Lachnospiraceae_unclassified
Clostridium
Rikenellaceae_RC9_gut_group
Firmicutes_unclassified
Eubacterium]_xylanophilum_group
Tyzzerella
Anaerotruncus
Candidatus_Stoquefichus
Harryflintia
Butyricicoccus
Lachnospiraceae_UCG-006
Duncaniella
Ruminococcaceae_UCG-004
Christensenellaceae_R-7_group
Eggerthella
Alistipes
Bifidobacterium
Prevotellaceae_UCG-001
UBA1819
Erysipelotrichaceae_unclassified
Ruminococcus_1
Anaeroplasma
Ruminococcus
Ruminococcaceae_UCG-010
A2
Hydroferulic acid
(2xi,20beta)-2,20-Dihydroxy-3-oxo-12-ursen-28-oic acid
Mesoporphyrin IX
MGDG 16:0; MGDG(7:0/9:0)
2-(4-Methoxyphenyl)naphthalic anhydride
Sarcodon scabrosus peptaibiotic
Americanol A
7,8-dehydrosteganthanthin
Dodeca-2(E),4(E)-dienoic acid
Plasmenyl-PC 36:6; PC(P-14:0/22:6)
8-Isoprostaglandin F2
Thiamine
Succinic acid
Ursocholic acid
Diacetolol
TG 66:21; TG(22:7/22:7/22:7)
Ethoxyquin
3a,6b,7b,12a-Tetrahydroxy-5b-cholanoic acid
TG 68:11; TG(20:5/22:5/26:1)
1,1'-[1,12-Dodecanediylbis(oxy)]bisbenzene
5-Hydroxyindole-3-acetic acid
1H-Indole-1-acetic acid
3-Methyldioxyindole
ar-Turmerone
Azelaic acid
Citalopram
Docosatrienoic acid
Enterolactone
FAHFA 27:3; FAHFA(5:0/22:3)
Ganoderic acid A
Indole
Indole-3-carbinol
Miltefosine
Naltrexone
Oleamide
O-Desmethylangolensin
Oleoyl-L-carnitine
Olmesartan medoxomil methyl ether
Tryptophyl-Tryptophan
Undecanedioic acid
D
Azelaic acid
1H-Indole-1-acetic acid
FAHFA 27:3; FAHFA(5:0/22:3)
Citalopram
Naltrexone
Miltefosine
Oleamide
Firmicutes_unclassified
Clostridium
Lachnospiraceae_unclassified
Harryflintia
O-Desmethylangolensin
Oleoyl-L-carnitine
Clostridiales_unclassified
Tyzzerella
Docosatrienoic acid
Eubacterium]_xylanophilum_group
Butyricicoccus
3-Methyldioxyindole
Lachnospiraceae_UCG-006
Bilophila
Enterolactone
Ganoderic acid A
Candidatus_Stoquefichus
Akkermansia
Tryptophyl-Tryptophan
Rikenellaceae_RC9_gut_group
Anaerotruncus
Indole-3-carbinol
Undecanedioic acid
Indole
5-Hydroxyindole-3-acetic acid
Olmesartan medoxomil methyl ether
ar-Turmerone
E
WBC
Absolute cell number per leg (×10^7)
Control
Tryptophan
I3C
F
WBC
n.s.
Absolute cell number per leg (×10^7)
Control
Indole
Indole-acetic acid
Indole-butyric acid
G
LSK count
n.s.
Absolute cell number per leg (×10^5)
Control
Tryptophan
I3C
H
ST-HSC count
Absolute cell number per leg (×10^5)
Control
Tryptophan
I3C
I
MPP count
n.s.
Absolute cell number per leg (×10^5)
Control
Tryptophan
I3C
J
LT-HSC count
n.s.
Absolute cell number per leg (×10^5)
Control
Indole
Indole-acetic acid
Indole-butyric acid
K
Control
Tryptophan
I3C
CD45.1
CD45.2
CD45.2+ 42.3 ± 3.6
CD45.2+ 58.2 ± 3.7
CD45.2+ 51.3 ± 4.6
L
Percentage(%)
Myeloid cell
B cell
T cell
Control
Tryptophan
I3C
M
Absolute cell number per leg (×10^4) (Donor derived)
Control
Tryptophan
I3C
CLP
CMP
GMP
MEP

Supplemental Figure 6. FMT-YA mice harbored a distinct metabolite landscape compared with FMT-AA mice, related to Figure 7. (A-B) Relative metabolite level in PB and BM plasma between FMT-AA mice and FMT-YA mice (n=6 per group). (C) Heatmap showing the correlation of differential microbiota and differential metabolites. Red indicated positive correlation; Blue indicated inverse correlation. (D) Correlation network between altered metabolites (blue) and differentially abundant microbiota (green). Lines between two nodes indicated correlated interactions, while red represented higher correlation, blue represented lower correlation. (E-F) Count of WBCs in BM from mice treated with tryptophan, I3C, indole, IAA or indole-butyric acid (n=5-6 per group). (G-J) Absolute number of HSPCs, LT-HSCs, ST-HSCs and MPP in BM among groups (n=5-6 per group). (K) Representative flow cytometry plots of donor-derived $CD45.2^+$ reconstitution in $CD45.1^+$ mice in HSC transplantation assay. (L) Proportions of donor-derived B cells, T cells and myeloid cells in PB at 4 months post HSC transplantation (n=6 per group). (M) The absolute cell number of donor-derived CLPs, CMPs, GMPs and MEPs in BM from recipient mice in HSC transplantation assay (n=6 per group). Graphs show mean ± SEM, with statistical significance determined by unpaired student's t-test. *$P < .05$, n.s., nonsignificant.